Evaluating conditional density estimation networks as a probabilistic downscaling tool: Application to precipitation in Newfoundland

by

© Biswas, Rasel
B. Sc.(Hons), M. Sc.

A report submitted to the
School of Graduate Studies
in partial fulfillment of the
requirements for the degree of
Master of Science.

Department of Scientific Computing
Memorial University of Newfoundland

21st June 2015

St. John's Newfoundland

Abstract

The objective of this research is to better quantify the distribution of extreme precipitation within Newfoundland, for the current climate conditions. The province of Newfoundland is interested in this information as guidance for climate adaptation and longterm infrastructure planning purposes. Extreme analyses are commonly limited by short periods of observation (often only 30 years or less), resulting in large uncertainty regarding rare events. These limitations can be addressed by increasing the period of observation, or partially addressed using synthetic time series generated by stochastic weather generators. These weather generators attempt to replicate relevant statistics of the observed climate, using various statistical modelling tools. Here, a probabilistic neural network-based downscaling method is used to predict the probability distribution of precipitation at a study site conditional upon the synoptic state of the atmosphere; that is, features of a given day's large-scale atmospheric state are used to estimate the likelihood of all possible precipitation amounts for that day. My results show that CDEN-based probabilistic downscaling generally agrees better with observations than uncorrected reanalysis-based precipitation estimates. However, it gives significantly higher estimates for extreme events at low frequency (e.g., 100 year return periods). This approach is demonstrated for St. John's airport. Comparison with nearby stations, Windsor Lake, suggests that these higher estimates may be reasonable; however, further work and a longer observational record is needed

to determine whether these estimates represent added value to the raw observational record or a shortcoming of our CDEN-based methodology.

Contents

List of Tables

List of Figures

Chapter 1

Introduction

The response of precipitation to climate change has been the subject of numerous studies, including annual and seasonal analyses on both global and local scales (Houghton et al., 1996). Past studies suggest that mean global precipitation has increased throughout the 20th century; however, trends show considerable spatial variability (Houghton et al., 1996). For example, in northern Europe, positive trends have been identified (Forland et al., 1996; Sc̈honwiese et al., 1997), while in parts of the south trends are often negative (Sc̈honwiese et al., 1997). This variability is partially explained by the complexity of precipitation responses to changing climate, which may include adjustments in the frequency of events, the intensity of events, or both (Trenberth et al., 2003; Allen & Ingram, 2002); furthermore, these responses may vary across the seasons (Finnis et al., 2007).

Impacts of climate change on intense, but relatively rare, periods of precipitation are especially of interest. These extreme precipitation events arise from complex interactions between temperature, moisture, winds and orography; individual extreme events typically influence small areas, making it difficult to predict the response of extremes to climate change. The biggest obstacle in this area of research is a lack of

high quality data with which to constrain results. At the end of the last century, a significant positive trend in the frequency of extreme rainfall (greater than 50mm per day) has been identified in the US (Karl et al., 1995, 1998). In Australia, a significant increase in the 90th and 95th percentiles of daily precipitation was identified by Suppiah & Hennessy (1995) and Suppiah & Hennessy (1998). Hennessy & Suppiah (1999) and Plummer et al. (1999) further showed increases in the 99th percentile.

A study by Groisman et al. (1999) provides a useful synopsis of precipitation responses to climate change, both on global and regional scales. Over the past century in the US, Australia, and Norway, Groisman et al. (1999) found that total annual precipitation had increased, as had the mean intensity of individual precipitation events, i.e., increasing intensity was contributing to an increase in precipitation amounts. In order to describe these changes, they compared fitted probability distributions under warmer and cooler climates; results suggested that parameters associated with the spread of a distribution (e.g., scale parameters) were most affected by warming, while those associated with the shape of a distribution were less affected. This translates to an increase in the likelihood of high precipitation amounts. These changes are independent of total precipitation; however, some locations (e.g., Siberia) experienced this increase in intensity without an associated increase in total precipitation, suggesting a compensating decrease in the frequency of events. Generally, however, the projected increases in total accumulated precipitation were found to be more robust than changes in extreme (intense) precipitation (Groisman et al., 1999).

A further problem in predicting climate responses to climate change involves geographic scale. While the general circulation models (GCMs) typically used for climate change analyses perform reasonably well over large spatial scales (e.g., 100-1000km), they do not adequately represent the small (regional or local) scales of greatest interest in climate adaptation planning. This issue compounds problems associated

with spatial variability of precipitation, as small-scale factors such as local topography, coastline orientation, and slope aspect (among many others) can exert large influences on local-scale precipitation, but cannot be captured by GCMs. The heaviest (most intense) precipitation events are also typically associated with processes acting on spatial scales much smaller than GCM resolutions; consequently, heavy precipitation is reduced as the impact of small-scale, intense events, such as convective storms, are spread over a very large GCM grid cell. Despite these limitations, large-scale GCM output can be used to infer local-scale impacts, assuming that a location's precipitation is adequately connected to large-scale forcing. The process of predicting local-scale information from large-scale data is referred to as 'downscaling', and is accomplished through a wide range of techniques (e.g., Benestad et al., 2008). Broadly, these fall into two categories:

i. Dynamic downscaling, in which higher resolution regional climate models are nested within low resolution GCM output, and

ii. Statistical downscaling, which capitalize on long observational records to identify cross-scale statistical relationships.

There is no single, universally accepted approach to precipitation downscaling, despite a number of comparative studies (e.g., Wigley et al., 1990; Wilby et al., 1998) and dedicated dynamical downscaling efforts (e.g., Christensen et al., 2007; Goodess, 2011; Gutowski et al., 2010). Commonly used statistical methods include transfer functions (e.g., regression) (Wigley et al., 1990; Wilby et al., 1998) and weather typing schemes (e.g., Vrac et al., 2007). Perfect prognosis methods (or, model output statistics) have been adapted for downscaling projections (Rummukainen, 1997), as have artificial neural networks (ANNs).

In order for statistical downscaling to be effective, the GCMs being downscaled

must simulate required large-scale variables realistically. When a direct relationship between large-scale variables is simulated by a model, and local-scale observations exist, statistical downscaling essentially corrects for model errors (see, e.g., Lenderink et al., 2007). Most downscaling methods are deterministic, that is, they provide a single 'best-guess' of precipitation given large-scale conditions. However, the same data used to identify and train downscaling models can be used to develop stochastic weather generators. These are statistical models that generate synthetic time series of the local scale variable while reproducing statistical properties of the observations (e.g., Wilks, 1998; Vrac et al., 2007). Incorporating stochastic weather generators into downscaling schemes has the potential to improve representation of extreme events (which are often the primary concern in adaptation planning); deterministic approaches frequently underestimate these extremes as they strive to predict the most likely outcome, which is often closer to the long-term mean value (e.g., Fowler et al., 2007).

Multivariate linear regression (MLR) forms the basis of the most commonly used statistical downscaling approaches. However, the interest in nonlinear regression methods, including ANNs, is increasing because of their potential to accommodate complex, nonlinear and time-varying input-output mapping. Relative to MLR, ANN-based regression is extremely flexible and capable of identifying nonlinear relationships between input (predictors) and output (predictands), given enough training data.

If no nonlinear relationship exists, ANNs give similar results to MLR-based methods, but with additional computational costs, and using a regression methodology that is much more difficult to interpret (Schoof & Pryor, 2001). However, when applied to precipitation, ANNs are often able to account for heavy rainfall events missed by linear regression approaches (Weichert & Buŕger, 1998). Cannon & McKendry (2002)

found that an ensemble ANN downscaling model was capable of predicting changes in stream flows using only large-scale atmospheric conditions as model input. Other nonlinear downscaling methods have been used, to varying effect. These include (but are not limited to) dynamic neural networks, which accommodate time-varying input-output relationships (Gautam & Holz, 2000), and Gaussian Processes (e.g., Cai et al., 2006). A common thread in these analyses is that nonlinear approaches typically offer better performance relative to MLR, at the cost of increased complexity. This is particularly true in locations where environmental processes are complex and highly nonlinear (Hsieh, 2009).

The multilayer perceptron (MLP) is the most common ANN used in statistical downscaling, and essentially acts as a nonlinear alternative to MLR. MLP can deal with unspecified interactions between multiple covariates to provide a deterministic prediction. An alternative approach uses a conditional density estimation network (CDEN), which is a probabilistic extension of the MLP (Gardner & Dorling, 1998; Hsieh & Tang, 1998; Dawson & Wilby, 2001). CDENs have been successfully applied to various prediction problems, including air pollutant concentration estimations (Dorling et al., 2003) and hydroclimatology (Haylock et al., 2006; Cannon, 2010). Rather than predicting the most likely outcome, a CDEN predicts probability distribution parameters, conditional upon the state of predictor variables. As such, it provides a more detailed prediction, allowing the likelihood of all outcomes to be quantified. When used in precipitation downscaling, its output can be considered as probabilistic downscaling.

The current study applies the CDEN method to precipitation in St. John's, Newfoundland. The purpose is to assess the method's suitability for climate projection analyses in the province of Newfoundland and Labrador. Here, a CDEN-based model is used to produce a conditional precipitation distribution for a modern study period.

Drawing randomly from these distributions produces an extended precipitation time series. This can be considered a conditional stochastic weather generator. The skill of the CDEN is assessed against available observations, and the approach is then used to estimate the magnitude of extreme events at our study location. The methods potential value in climate projection is assessed on the basis of this analysis. Subsequent chapters describe this method in detail. In the current study, extreme value statistics are based on annual maxima (a 'block maxima' approach, rather than a peaks-over-threshold approach). This was chosen to better emulate the methods used by Environment Canada for their official intensity/duration/frequency (IDF) analyses.

Chapter 2

Data

2.1 Overview

All analyses are based on freely available data sets from Environment Canada and the U.S. National Centers for Environmental Prediction (NCEP). Predictor variables (i.e., inputs to downscaling algorithms) were taken from the NCEP/NCAR Reanalysis (Kalnay et al., 1996), while predictand (output) variables are from the Adjusted and Homogenized Canadian Climate Data set (AHCCD; Vincent, 1998).

2.2 Atmospheric Reanalyses

The need to monitor climate and weather arises for a variety of reasons, from short-term planning and hazard preparedness to long-term infrastructure planning (e.g., using intensity-duration-frequency curves for precipitation). Climate observing stations are our primary tool in this effort, providing detailed descriptions of climate at fixed locations. However, maintaining these observing sites is expensive, and coverage is largely limited to populated land areas. Satellite observations can help fill

gaps in the surface observing network, but provide less detailed coverage (varying spatial/temporal coverage), and often provide only indirect measurement of many variables of interest (Climate Change Science Program, 2008).

Reanalyses were originally proposed as a means of addressing the shortcomings of climate station and satellite-based observations. This approach was inspired by the use of atmospheric analyses in meteorology, i.e., the merging of current observations and prior model forecasts into a best-guess of the atmospheric state at a given point in time. In operational meteorology, analyses provide a starting point for numerical weather prediction (NWP) models. The approach used to generate analyses evolves continually as data assimilation and modelling techniques improve, complicating efforts to interpret long-term climate using incompatible analyses. Reanalyses address this consistency issue, creating a continuous record using a single NWP model and data assimilation methodology. The result is a gridded data set of all "analysed" variables with global coverage over the reanalysis period (usually ∼1950s to present). In essence, reanalyses estimate data at locations away from climate stations or satellite observations using a combination of all available observations at other locations and model output; effectively, it provides an intelligent interpolation informed by NWP physics. Variables that are not directly analysed can be provided by subsequent iterations of the NWP model (referred to as reanalysis forecast variables) (Kalnay, 2003). Reanalysis data has proven consistent with the trends produced from the other observational datasets with some regional exceptions, especially since satellite measurements originated in the late 1970s (Climate Change Science Program, 2008). Unfortunately, reanalysis treatments of precipitation are often of poor quality relative to other variables (e.g., temperature or sea level pressure). The primary factors that are responsible for this inconsistency in the trends are limitations in the models and the methods used to integrate the datasets (Bromwich & Cullather, 1998). Nevertheless,

reanalysis data helps to identify and explore atmospheric features associated with the weather and climate variability. Reanalysis can assist in these efforts by providing large-scale context for events such as droughts or floods, allowing us to move beyond studies at fixed locations.

2.3 Station data

Station data used in the current study were taken from the Adjusted and Homogenized Canadian Climate Data archive (Vincent, 1998; Vincent & Gullett, 1999; Vincent et al., 2002; Mekis & Vincent, 2011). This was used in place of raw (unadjusted) station data, as the influence of factors such as station relocation, changes in observational practices, and instrument replacement have been removed in the AHCCD. We have used daily precipitation values; total precipitation accumulated in a 24 hour period (mm). It is calculated as the addition of the station's adjusted daily rain gauge and snow observations (converted to water equivalent). AHCCD development is a continuous process, and adjusted precipitation is updated every year, making it easy to update or extend our analysis with new data as it becomes available.

Chapter 3

Methodology

3.1 Neural networks

Inspired by the mechanics of biological learning, artificial neural networks (ANNs) are a family of computational algorithms commonly used for classification and regression problems. Capable of identifying nonlinear relationships between various parameters, they are well suited to statistical modelling and prediction in the environmental sciences. Although building neural networks ("training") can be an involved process, and resulting models are often very complex, many easy-to-use software packages are now available that simplify the process for users with limited formal statistical training.

In the most common approach to training, a neural network is iteratively shown paired inputs (predictors) and desired outputs (predictands). This is referred to as supervised training, as the network is guided towards a known outcome (i.e., the predictand); it is distinct from unsupervised training, which excludes information regarding outputs (i.e., no prior information regarding outcomes). In the course of supervised training, a network adapts to minimize differences between its predictions

and supplied outputs. Essentially, the network assumes a relationship exists between supplied inputs and outputs, and attempts to capture it. Supervised NNs are commonly used as nonlinear analogs of traditional multivariate linear regression.

The goal of training is to optimize the NN's parameters, which are a series of weights (w) and biases (b). The number of parameters and structure of the final network are set by a user prior to training; a description of how weights and biases are structured is provided in Section 3.2.

3.2 Multilayer perceptron (MLP)

Each iteration of the training process adjusts the weights by a small amount. Suppose the training process is in its m^{th} iteration; when shown the $(m+1)^{th}$ set of paired predictors and predictands, the weights may be updated in the following way:

$$w_{ij}^{m+1} = w_{ij}^{m} + \Delta w_{ij}^{m}, \tag{3.1}$$

where Δw_{ij}^{m} is the updated weights. The multilayer perceptron (MLP) is a common neural network model, belonging to the class of supervised networks. Using historical data, the MLP network is capable of effectively mapping output data to input data (i.e., they may be used for classification or regression). The MLP consists of layers of 'nodes'; the number of layers and number of nodes per layer are set by the user prior to training. All MLPs include an input layer (which accepts predictors as input), an output layer (producing desired predictands), and an arbitrary number of 'hidden' layers, so named because the value of nodes in these layers is not typically examined or relevant to the user.

Mathematically, a trained MLP can be described as follows. Let

$$F : X \rightarrow H$$

be a simple mathematical model which represents the first layer of MLP mappings, where X represents the predictor set (inputs), H represents the first layer of MLP nodes, and F represents the activation function or transfer function connecting the nodes input layer to the hidden layer. The transfer function F can be linear or nonlinear. The hyperbolic tangent function and unipolar sigmoid functions are commonly used nonlinear transfer functions. Let $x_i\,(i = 1, 2, ..., I)\,\epsilon\, X$ be a given set (i.e., input set) that will produce a value for $h_j\,\epsilon\, H$ determined by set weights $(w_{j,i})$ and biases (b_j) connecting it to input values; here, j gives the number of nodes in this first hidden layer.

The value of the j^{th} node (h_j), is then calculated as follows:

$$h_j = F\left(\sum_i x_i\ w_{j,i} +\ b_j\right) \tag{3.2}$$

That is, h_j is a function of all inputs x_i. For an MLP with only a single hidden layer, the values of H then determine the values of the output layer O:

$$g : H \rightarrow O.$$

Suppose $o_k\,\epsilon\, O$ and let g_k be the transfer function, which is often chosen to constrain output within a specified (e.g., physically meaningful) range. Now, h_j is the output from the first input layer, which is multiplied by the interconnected weights $w_{k,j}$ and b_k is the bias for the output layer. Then

$$o_k = g_k\left(\sum_j h_j\ w_{k,j} +\ b_k\right) \tag{3.3}$$

Again, the outputs are a function of all nodes in the hidden layer. For MLPs with multiple hidden layers, nodes in subsequent layers are determined by the value of

nodes in the previous layer. If the multilayer perceptron is too complex (i.e., with many hidden layers), this may lead to over-fitting by incorporating the noise, and not just the desired signal, into predictions. When compared to training data, over-fitted MLP output will show extremely high agreement with actual outcomes; however, they will show poor performance when used to predict novel data points not used in the training period. For this reason, MLP performance must always be evaluated using 'testing' data, independent of training data (Hsieh, 2009).

3.3 The Conditional Density Estimation Network (CDEN)

The CDEN is a probabilistic extension of the classical MLP. Rather than returning the single, deterministic value provided by the standard MLP, a CDEN returns probability distribution parameters, conditional upon input variables. Training of the network proceeds in a similar fashion to the traditional MLP, with some adjustment to the standard cost functions. The current study uses the algorithm described in Cannon (2008). The goal is to identify the NN's parameters such that the resulting conditional distribution maximizes the probability of the training dataset, rather than minimizing the error of NN predictions. The CDEN assesses the likelihood of actual outcomes against a predicted probability density function; as the probability of the true outcomes increases, the cost function is optimized. A description of this optimization approach follows.

Suppose x is a continuous sample of data with known probability distribution, $f(x, \theta_i)$, where $\theta_i, i = 1, 2, 3, ..., n$ are the unknown constant NN weights and biases (hereafter referred to as NN's parameters, distinct from statistical distribution parameters) to

be estimated from the sampling data. The likelihood function L is a map

$$L : \Theta \rightarrow \mathbb{R}$$

which is given by

$$L(x \mid \theta_i) = f(x \mid \theta_i); \theta_i \epsilon \, \Theta_i, \; i = 1, 2, 3, ..., n$$

where Θ is the parameter space. If $x_1, x_2, ..., x_n$ are independent observations then the likelihood function can be written as

$$L = L(x_1, x_2, ..., x_n | \theta_1, \theta_2, ..., \theta_n) = \Pi_{i=1}^{n} \, f(x_i | \theta_1, \theta_2, ..., \theta_n). \tag{3.4}$$

Taking the natural logarithm of both sides, then

$$In \, L = \sum_{i=1}^{n} In \, f(x_i | \theta_1, \theta_2, ..., \theta_n). \tag{3.5}$$

Now, the maximum likelihood estimates of $\theta_1, \theta_2, ..., \theta_n$ are obtained by maximizing L or $In \, L$. By using the definition of critical point, we can write

$$\frac{d \, In \, L}{d\theta_j} = 0; \;\; j = 1, 2, ..., n \tag{3.6}$$

The solution of unknown parameters $\theta_j \, (j = 1, 2, 3, ..., n)$ is found by solving the above system of equations. When using the likelihood function, f is set to a known probability distribution. In the current study, the Bernoulli-gamma distribution has been used, with three distribution parameters.

$$L \; = \; \Pi_{i=1}^{n} \, p(y_n \mid p_n, \alpha_n, \beta_n) \tag{3.7}$$

where

$$p(y_n \mid x_n) \; = \; p(y_n \mid p_n, \alpha_n, \beta_n)$$

and $p_n = f(x_n)$, $\alpha_n = f(x_n)$, $\beta_n = f(x_n)$ are CDEN outputs; that is, probability distribution parameters vary with the input vectors. Minimizing the negative log of the likelihood function is equivalent to maximizing the likelihood function. Hence, the objective function is

$$J = -\sum_{n=1}^{n} In\ p(y_n|w,\ x_n)$$

Since x_n and y_n are known from the given data, the unknown w is optimized to minimize J.

3.4 Predictor selection method

When building statistical models, it is very important to select a set of appropriate input feature variables. The objective is to find the smallest set of features that ensures satisfactory predictive performance. With sufficient time and computing power, this can be accomplished by training multiple prediction/downscaling models using every possible combination of predictors, then using the single model that gives the best performance. However, this is not feasible if

i. very large numbers of potentially useful predictors are available, and/or

ii. training takes significant computing resources.

In these situations, an alternate (and faster) prediction method may be used to test all predictors first. Decision trees are often used for this purpose. These are computationally efficient tools that can be trained quickly, but have limited predictive power relative to systems such as neural networks; for example, decision trees cannot extrapolate outside the range of output data supplied during training (SAS Institute

Inc., 2011). The process partitions the entire output data set into multiple disjointed subsets, and then fits single responses into each individual region of the tree. The tree is built by finding the input variable that best splits the output data into two groups, and then, after separating the data, this process is applied to each sub-group separately. The process is continued until the subgroups either reach a minimum size or until no improvement can be made. The earlier and/or more often a given input variable is selected as the basis for division, the more likely it is to be a useful predictor. Here, Recursive Partitioning and Regression Trees (RPART) have been used to screen candidate predictors. These included functions of day of year, sea level pressure (psl850), relative humidity (rh850), specific humidity (sp850), temperature (t850) for 850mb, vertical velocity (v500), and geopotential height (z500) fields for 500mb from NCEP reanalysis for the fifteen nearest points to St. John's. Locations are shown in Figure 3.1. The nearest and furthest point is 19km and 476.59km respectively from St. John's airport.

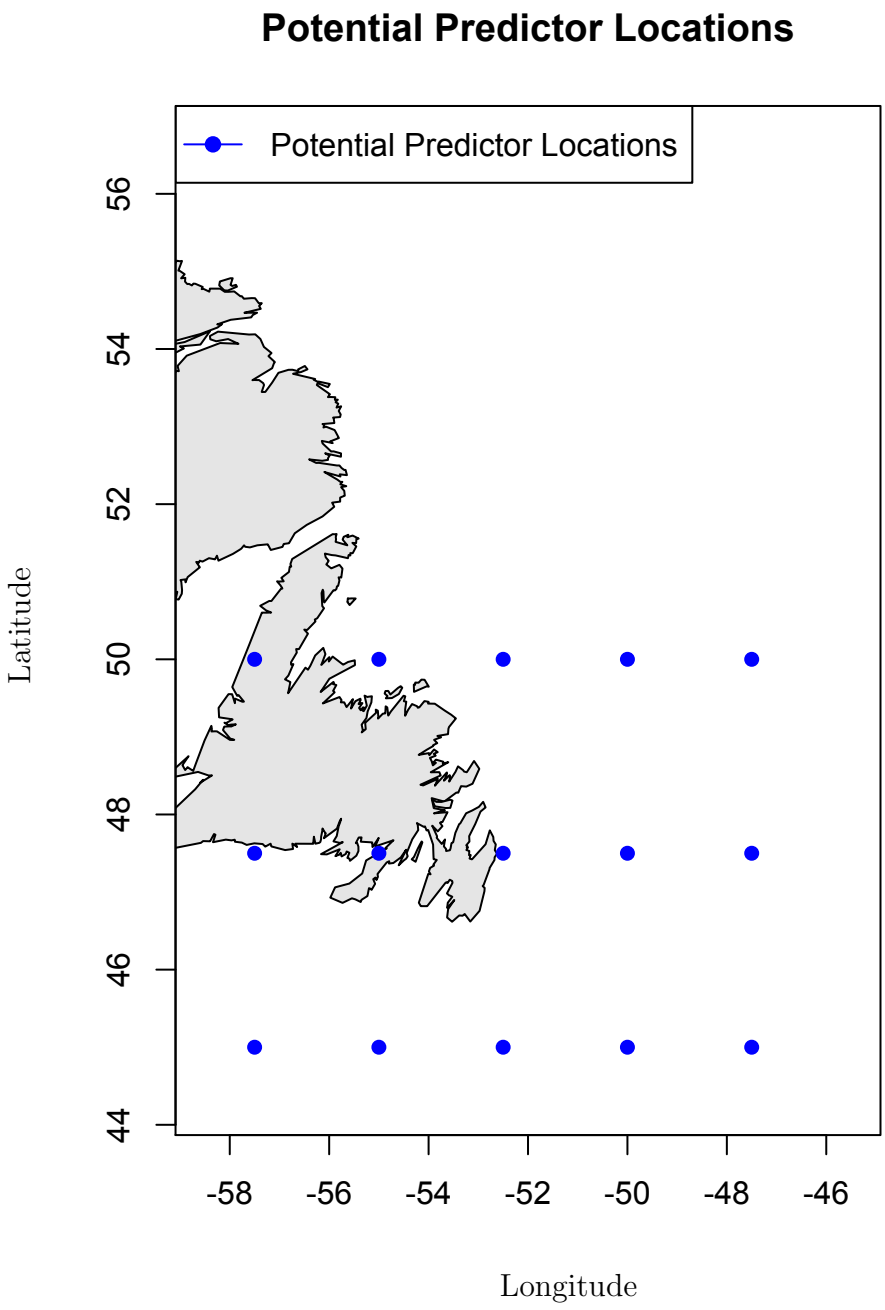

Figure 3.1: Potential predictors from NCEP reanalysis at locations used in the current study.

3.5 Probability distributions for daily Precipitation

In order to apply the CDEN methodology to precipitation downscaling, a suitable probability distribution for precipitation at the target location must be selected. A common choice for daily precipitation totals is the mixed Bernoulli-gamma distribution, in which a probability of zero precipitation is combined with a gamma distribution for non-zero precipitation probabilities (e.g., Williams, 1998; Haylock et al., 2006; Cawley et al., 2007; Cannon, 2008). The current study also adopts the Bernoulli-gamma distribution for St. John's, having confirmed the distribution is suitable for this region. Figure 3.2 compares a histogram of St. John's daily precipitation to a histogram of randomly sampled data from a Bernoulli-gamma distribution fitted to this same St. John's data.

The Bernoulli-gamma distribution has three specified parameters; a probability of precipitation occurring (p), a shape parameter (α), and a scale parameter (β). Its probability density function is

$$f(y; p, \alpha, \beta) = \frac{p\,(\frac{y}{\beta})^{\alpha-1}\,exp(\frac{-y}{\beta})}{\beta\Gamma\alpha},\ if\ y > 0$$

and

$$f(y; p, \alpha, \beta) = 1 - p,\ if\ y = 0$$

where y denotes the amount of precipitation. The mean and variance of the distribution are given respectively as

$$\mu = p\,\frac{\alpha}{\beta}$$

and

$$s = p\,\alpha\,\left(\frac{1 + (1-p)\alpha}{\beta^2}\right).$$

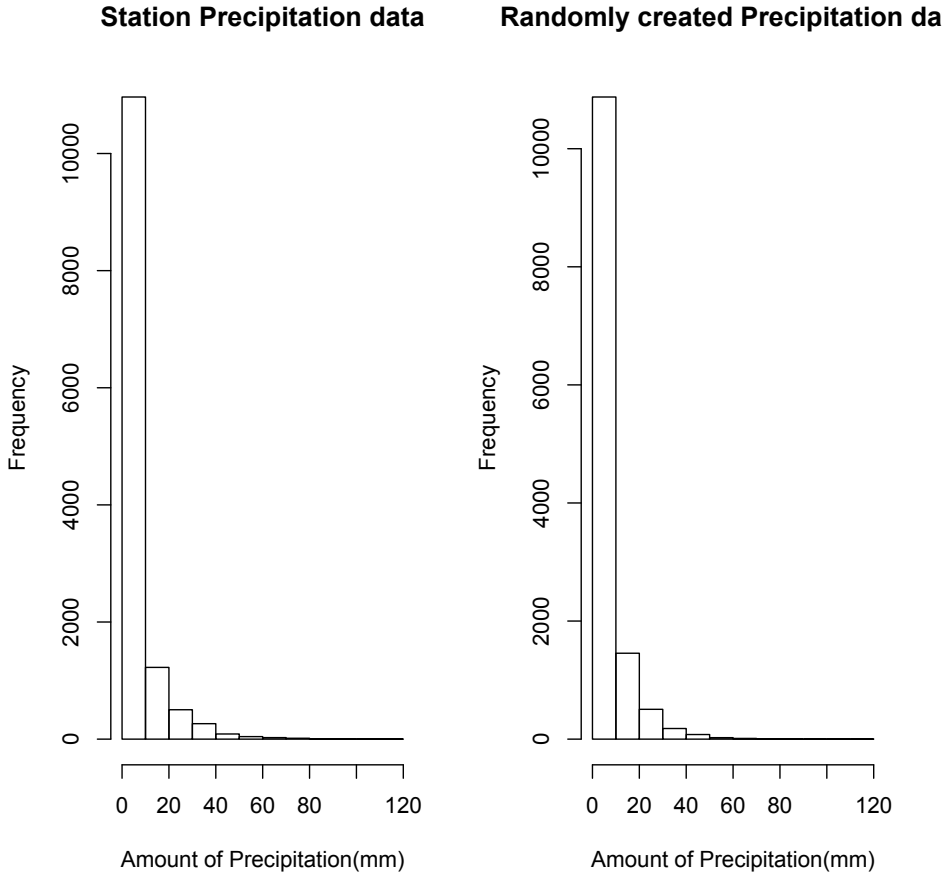

Figure 3.2: Station data and randomly created Precipitation data via Bernoulli-gamma distribution.

The current study uses a probabilistic downscaling approach, in which the parameters of a Bernoulli-gamma distribution are conditional upon daily large-scale forcing; that is, all three Bernoulli-gamma parameters are allowed to vary in response to daily conditions, reflecting changes in the likelihood that a given amount of precipitation will occur. For example, a properly trained CDEN should increase the likelihood of zero precipitation during synoptic conditions that promote clear skies, and increase the likelihood of heavy precipitation when conditions are extremely warm, humid,

and highly unstable. Daily CDEN-predicted distributions can then be used as a conditional weather generator, informed by daily large-scale variability; the distribution can be randomly sampled multiple times to identify a reasonable precipitation range for that day. This approach provides a greater depth of precipitation information than single-value deterministic downscaling, and better reflects daily variability than a weather generator based on a static daily precipitation distribution. So, the extreme events are identified as the maximum precipitation of each year. These extreme events are extracted from precipitation data and stochastic weather generator sample data.

3.6 Cross-Validation

When using any powerful empirical prediction technique, we must be careful to avoid over-fitting. This can be accomplished by excluding some data from training, allowing testing of the trained prediction algorithm against independent data. This is convenient if very long time series are available, but is difficult if only limited data is available. In this situation, cross-validation is often used to produce longer data sets for evaluation (e.g., Hsieh, 2009). Figure 3.3 illustrates how cross validation works. The process splits the data into a pre-selected number of segments. The data has been distributed equally among the segments; one segment is called the test data and the remaining segments are called the training data. An estimation of each segment is then produced by a prediction model trained with the remaining segments. In this way, the full time series of data is estimated by a series of independent models.

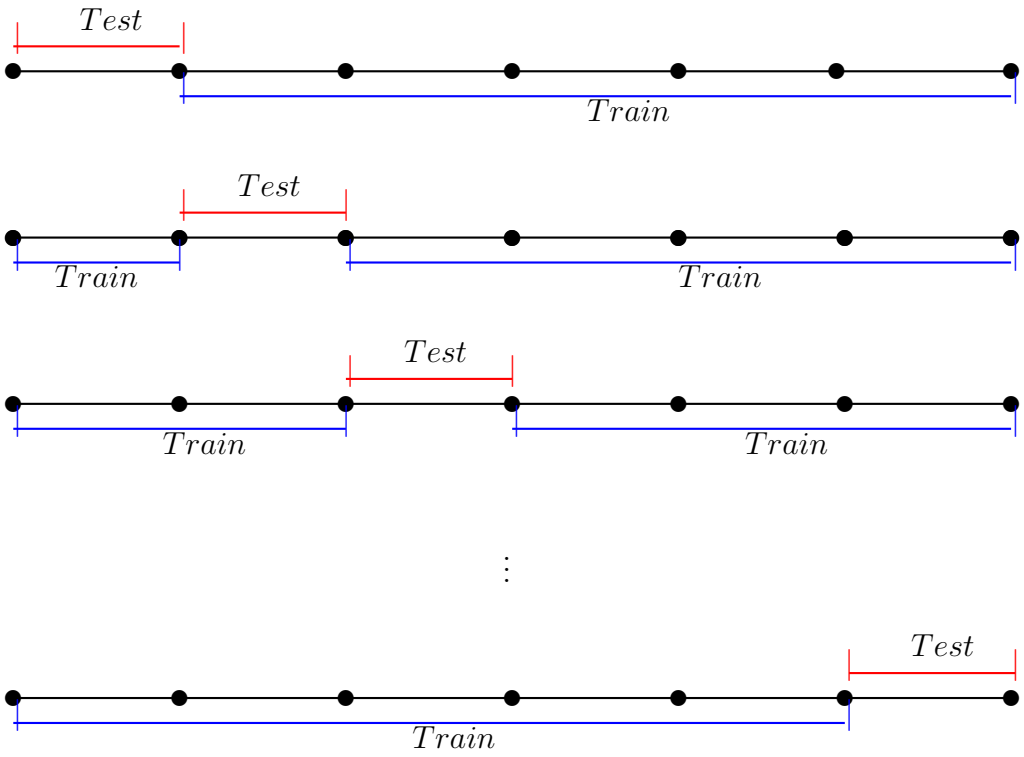

Figure 3.3: Cross Validation (CV) method.

Chapter 4

Application of Conditional Density Estimation Networks to Precipitation Downscaling in Newfoundland

4.1 Predictor Selection

The RPART predictor selection method used here is described in Chapter 3; here, it has been used to select between the following daily mean fields obtained from the NCEP reanalysis: sea level pressure (psl850), relative humidity (rh850), specific humidity (sp850), and temperatures (t850) recorded at the 850mb pressure level ($\sim$ 1km above sea level), and vertical velocity (v500) and geopotential height (z500) at the 500mb pressure level ($\sim$ 5.5km above sea level). Data from the fifteen NCEP grid points nearest the St. John's airport were included; these all lie within 450km of the airport. As the expected daily precipitation varies with the annual seasonal

cycle, sine/cosine representations of the seasonal cycle (as a function of day of year) were added as additional candidate predictors. The following additional predictors (variable and location given) were identified as relevant in an RPART analysis, and including in CDEN training: temperature at $(-47.5°, 47.5°)$, sea level pressure at $(-55°, 45°)$ and $(-55°, 50°)$, vertical velocity at five locations $(-52.5°, 47.5°)$, $(-50°, 47.5°)$, $(-55°, 47.5°)$, $(-55°, 45°)$ and $(-57.5°, 45°)$, and relative humidity at three different locations $(-52.5°, 47.5°)$, $(-55°, 47.5°)$, and $(-55°, 45°)$. In Figure 4.1, the blue points demonstrate the locations of the potential predictor parameters and the red points demonstrate the locations of the effective predictor parameters.

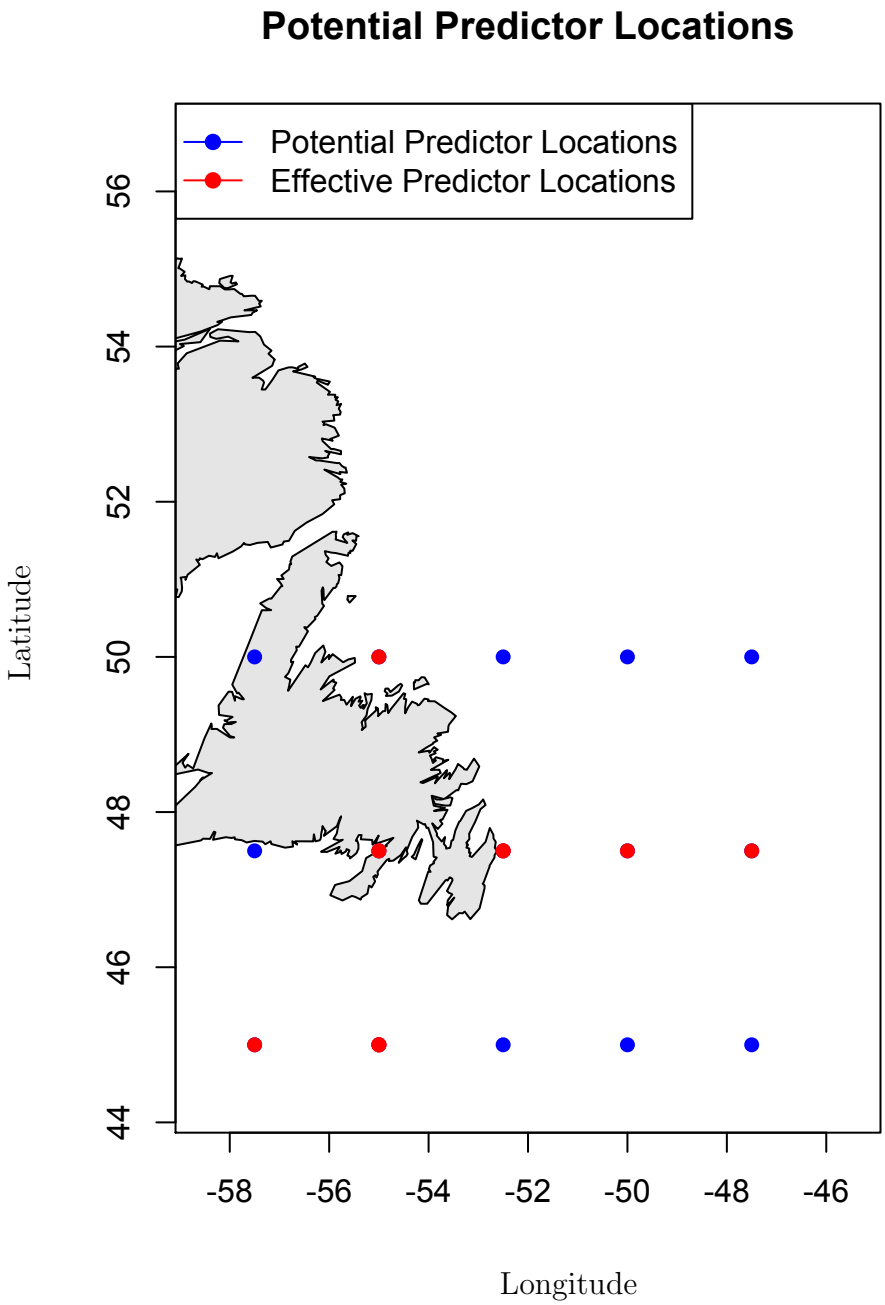

Figure 4.1: Red locations and blue locations represents selected predictor locations and potential predictor locations respectively for precipitation at the St. John's airport station.

4.2 Results and Discussion

The thirteen candidate predictors were applied in the CDEN training process. Daily data covering January 1^{st}, 1976 through December 31^{st}, 2011 were used. A six-fold cross-validation approach was adopted, in which the full 1976-2011 daily time series was separated into six equal segments. Daily precipitation for each segment was then simulated using a CDEN trained with the remaining five segments, ensuring the simulations were based on independent data. These simulations consist of daily Bernoulli-gamma probability distribution parameters, conditional upon the state of the thirteen predictor values: scale and shape parameters, along with the conditional probability of non-zero precipitation for the day.

In order to evaluate the performance of the CDEN, a 'best-guess' time series of daily precipitation was evaluated by comparing

i. the median of the daily CDEN-generated Bernoulli-gamma distribution to

ii. observed daily precipitation totals.

Table 4.1 summarizes results as a series of relevant skill scores (Wilks, 2006). As a comparison point, the same scores are presented for predictions for St. John's from the raw NCEP-NCAR reanalysis daily precipitation field. The reanalysis values give a benchmark for performance at our study location.

Table 4.1 shows the deterministic and categorical performance of the CDEN-derived 'best-guess' time series for St. John's; this represents a deterministic prediction by the trained CDEN model. Results show that the root-mean square error (RMSE) of the deterministic CDEN prediction is not significantly different from NCEP, consistent with results generated in other studies using a coupled ANN-analog downscaling model (Cannon, 2008). The correlation coefficient for both methods is statistically

Statistic	CDEN	NCEP
RMSE(mm)	**7.57**	7.97
r	0.62	.62
HIT	**0.90**	0.63
FAR	**0.13**	0.23
TSS	**0.77**	0.40
BIAS	**1.03**	0.82

Table 4.1: Cross-validated model performance statistics for CDEN, NCEP downscaling models with root mean square error (RMSE), correlation (r), Hit-rate (HIT), False alarm ratio (FAR), True scale statistic (TSS), Bias ratio (BIAS).

significant, but there is no difference between them. The remaining skill measures in Table 4.1 are based on categorical predictions; specifically, whether precipitation does or does not occur. Here, precipitation was considered to have occurred if a prediction (from the deterministic application of the CDEN or NCEP) gave a daily precipitation of 0.5mm or more. Four skill measures are considered:

i. the hit rate (HIT) gives the fraction of correctly forecasted events, with HIT = 1 being a perfect score;

ii. the false alarm ratio (FAR) gives the fraction of incorrect 'yes' forecasts (i.e., predicting an event that does not occur), with a perfect score of FAR = 0;

iii. the true skill statistic (TSS) is the difference between HIT and FAR, with 1 being a perfect score; and

iv. BIAS (B), calculated as the ratio between the number of times an event is predicted relative to the number of times an event occurs, with B = 1 being the

ideal score (Wilks, 2006).

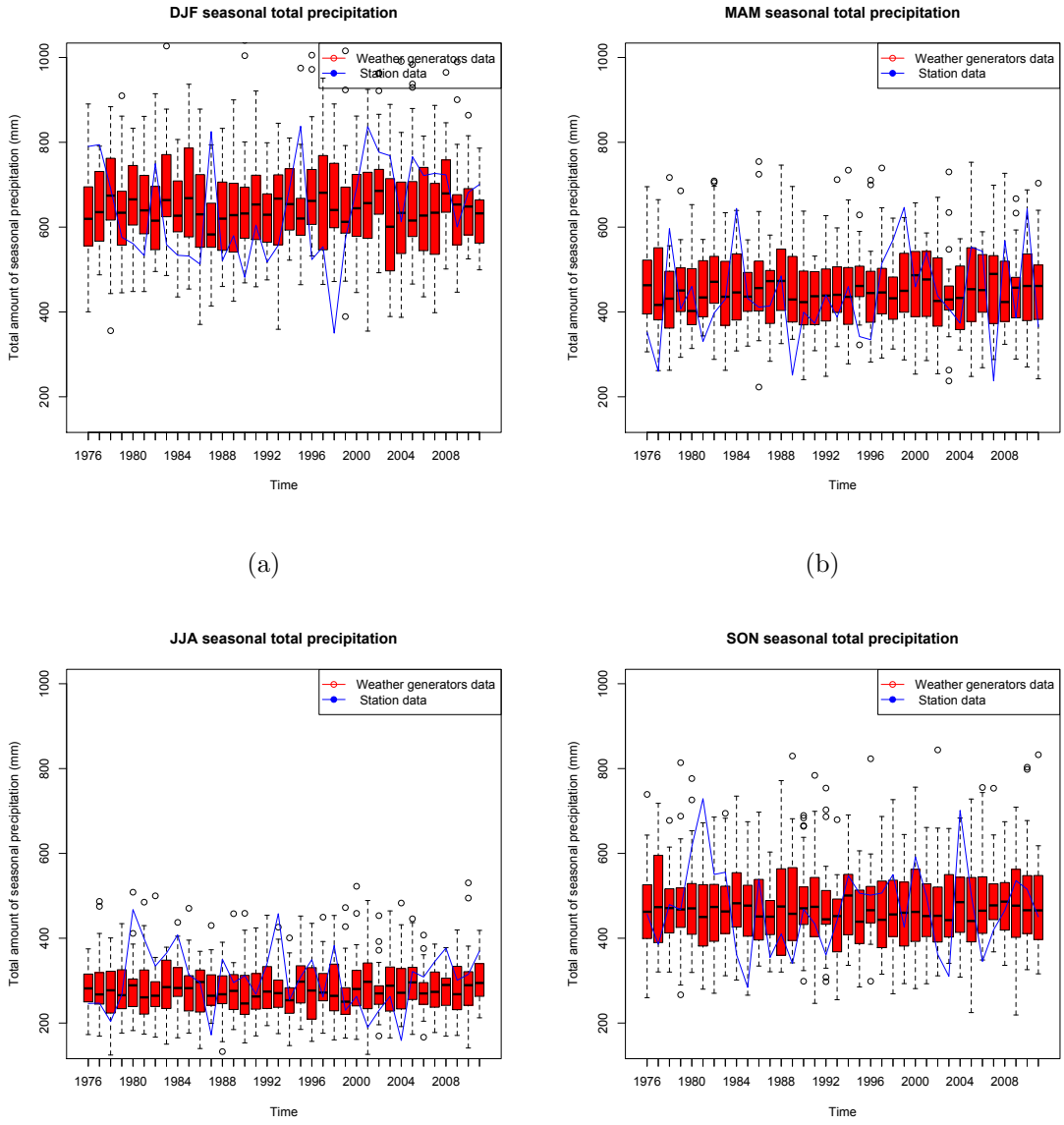

(a) (b)

(c) (d)

Figure 4.2: Compared total amount of seasonal precipitation between the station data and the stochastic weather generator using CDEN Model. The blue line represents the total amount of seasonal precipitation for the station data and box plot represents the total amount of seasonal precipitation for the stochastic weather generator.

Here, the CDEN predictions give significantly higher skills than NCEP predictions, with higher HIT, lower FAR, and better TSS. The CDEN model is a little over-biased, while NCEP is significantly under-biased (predicting too few events). Thus, we have found the CDEN model to be more effective than the NCEP in predicting whether precipitation will or will not occur, even if RMSE and correlation does not show significant differences. Figure 4.2 compares total seasonal precipitation from observations (blue line) to the 30-member ensemble generated with stochastic generator. Results show reasonable agreement, with seasonal totals usually remaining within the 95% confidence interval predicted by the model. There are several instances when observations and the model diverge significantly (e.g., Winter, 1998), although these are relatively rare. Along with results in Table 4.1, this plot emphasizes that the CDEN provides a reasonable, though imperfect, fit with observations.

In an attempt to further evaluate the strength of the CDEN approach to simulate

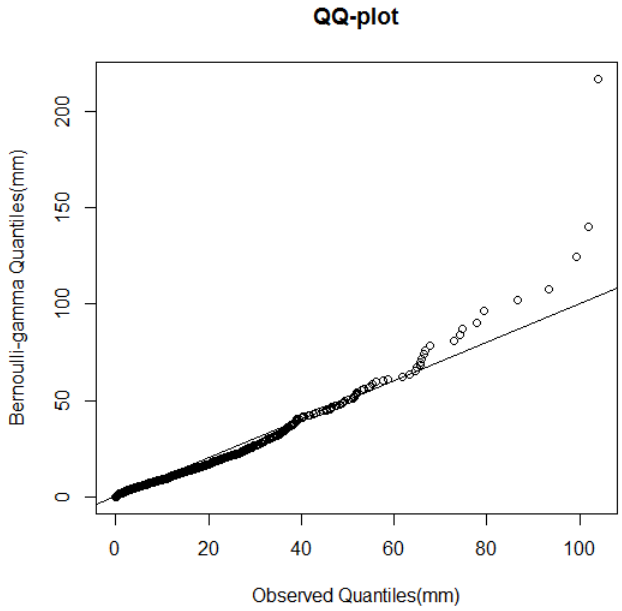

Figure 4.3: Quantile-Quantile plot at the St. John's international airport.

realistic precipitation fields, a quantile-quantile plot was produced (Figure 4.3). Here, the probabilistic potential of the CDEN approach is explored. Instead of drawing a single 'best-guess' from the daily CDEN-predicted precipitation distributions, 30 random samples were taken, providing a greater sense of each day's likely precipitation. The result is a CDEN-derived stochastic weather generator sample thirty times the size of the original observed time series. If the CDEN is well trained and works well, this stochastic sample should give a better sense of extreme precipitation events than a short observation time series. If the observation period is long enough, the two should give similar results.

Figure 4.3 compares quantiles of observed St. John's precipitation over the training period (horizontal axis) to quantiles from the CDEN sample (vertical axis). A reference line in this plot shows what perfect agreement would look like. From Figure 4.3, it is clear that there is a strong relationship between the observed test data and the simulated precipitation data for events lower than 70mm. This is a significant amount of precipitation, exceeded roughly once every 1.33 years in the observed data. Above 70mm, the quantile-quantile plot suggests the CDEN overpredicts precipitation amounts, with several large outliers. These outliers, or extreme events, are important events for climatology, and are used as design criteria in engineering infrastructure. Results suggest that either the CDEN stochastic sample overestimates these large events, or that the observational data underestimates them. Figure 4.4(a) shows the daily precipitation data of our observation site. In these figure, the x-axis represents the precipitation interval and the y-axis represents the amount of precipitation; that is, we have split observed precipitation into discrete categories ('intervals'; x-axis), then show the range of precipitation in that interval as a box and whisker plot (y-axis). This figure is presented to highlight aspects of extreme precipitation at this location; notably, the observational record shows that daily precipitation in

excess of 100mm occurs only four times in the period examined. These extreme outliers may have a strong impact on the training of the CDEN model, in either a negative or positive manner. Ideally, these rare events would provide information on conditions that promote extreme precipitation. However, with so few large events, the CDEN may not be able to accurately identify predictor/extreme precipitation relationships, leaving the CDEN unable to simulate these events realistically. This may be the case here, as the CDEN developed for this paper appears to over-estimate the magnitude of extreme precipitation relative to observations (Figure 4.3). Figure 4.4(b) shows the same information as Figure 4.4(a), but this time for a synthetic time series (CDEN output). Comparing these gives more insight into the CDEN's extreme overestimates. The larger stochastic sampling is thirty times the size of the original time series, allowing a closer examination of the CDEN's interpretation of rare events. Results again suggest the CDEN output overestimates the magnitude of large precipitation events. Comparing results in the high precipitation categories (>100mm) in Figure 4.4(a) and Figure 4.4(b), the CDEN tends to adopt much higher values, even reaching 216.7mm in the most extreme case. However, the CDEN accurately captures the relative frequency of extreme events, producing 131 events with 100mm or higher. Given that the stochastic CDEN sample is thirty times the size of the observation time series, this is a close match to observations (four events in 36 years, compared to 131 in 1080 simulated years). Respectively, these give a mean frequency of 0.11 and 0.12 extreme events per year, or return periods of 9 and 8.2 years.

The apparent tendency for the CDEN to 'overforecast' the magnitude of extreme events raises concerns that this statistical model is unsuitable for extreme precipitation analysis in our study region. Alternatively, results could be interpreted as an indication that very high precipitation events are more likely to occur here than the

raw observational record would suggest.

A recent extreme precipitation analysis conducted using a second data source suggests this may be the case, and that much larger precipitation events are possible than have been recorded at St. John's airport. Specifically, a rain gauge located 1.6km from St. John's airport (Windsor Lake) recorded three events that are greater than 100mm since 1998; respectively, these were 104.9mm, 149.6mm, and 180mm (CBCL Ltd., 2014). This later amount far exceeds the maximum (144.8mm) recorded at the airport, and suggests the CDEN's larger estimates are warranted (e.g., reasonably likely to occur). It is important to note that although the CDEN does simulate a handful of events larger than the maximum 180mm Windsor Lake measurement, they are very rare: in our 1080-year simulation, only 8 were recorded, giving a return period of 135 years.

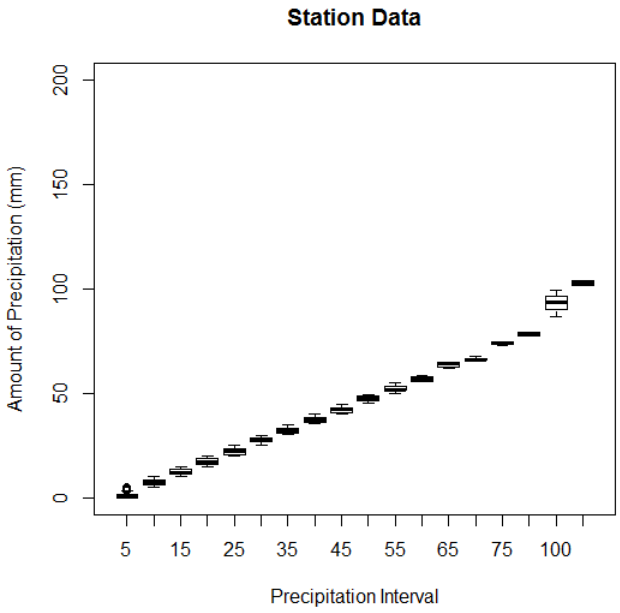

(a)

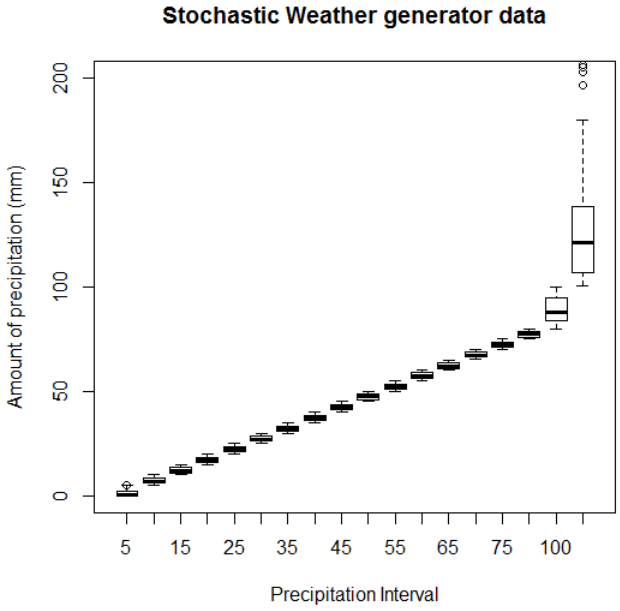

(b)

Figure 4.4: Compared between (a) the precipitation data for St. John's airport and (b) the stochastic weather generator using CDEN Model.The line inside each box represents the median, boxes extend from the 25th to 75th percentiles, and outliers are shown as circles.

4.3 Summary and Conclusion

Results indicate that the CDEN methodology, as applied in the current study, can offer some useful insight into local precipitation distributions and extreme events. However, they also suggest the method should be used with caution. As a precipitation downscaling method, the CDEN appears to work reasonably well, although it retains errors in magnitude comparable to NCEP/NCAR reanalysis estimates. The CDEN does, however, strongly outperform the reanalysis when predicting whether precipitation will or will not occur, with much better hit rates, bias, and false alarm rates. CDEN skill shown here is comparable to skill reported in similar studies of other locations (e.g., British Columbia; Cannon, 2008).

Although the reasonable performance as a deterministic downscaling technique confirms that our CDEN application is capable of capturing relationships between large-scale forcing and local scale precipitation (Table 4.1), the method is potentially more valuable as a tool for exploring the broader precipitation probability distribution and extreme precipitation events. To explore this potential, the CDEN was used as a conditional weather generator, generating a large synthetic precipitation data set by randomly sampling CDEN-based daily conditional precipitation distributions. In this case, each day in our 36-year study period was sampled 30 times, giving 1080 equivalent years of synthetic data. A comparison between the 36-station record suggests that the CDEN overestimates extreme precipitation values (Figure 4.3, 4.4). However, our ability to evaluate the CDEN is limited by the available observational record; with only 36 years examined, it is possible that this record is under-representing extreme events. This is supported by other nearby precipitation records, which include events much larger than those observed at St. John's airport over the same period of record (e.g., Windsor Lake, with a maximum of 180mm in 24 hrs). Keeping this

in mind, CDEN results suggest that design criteria like the 100-year return period should be increased relative to values based on observations alone. At present, however, it would be premature to base design criteria on CDEN output alone.

The novelty of the work is mostly in our application in a new geographic context, and reframing of the CDEN framework as 'probabilistic' downscaling. Computing challenges included

i. predictor screening/selection for St. John's,

ii. adaptation of the CDEN algorithm to the current context (including scripting and testing a new cost function in an existing CDEN package in R),

iii. application of a cross-validation methodology.

Further work on predictor selection and analyses based on longer data sets may be able to improve the skill of the CDEN predictions; this work is necessary for this technique to be truly useful for operational decision making. If improved CDEN skills are achieved, this tool may prove useful in projecting the impact of climate change on extreme precipitation in Newfoundland. By then applying a CDEN trained with observations and reanalyses to 20th and 21st general circulation model output, it would be possible to explore shifts in precipitation distributions in detail, even when only relatively short model runs ($\leq$ 100 years) are available. This is being considered for future work.

Bibliography

2008 Reanalysis and Attribution: Understanding How and Why Recent Climate Change Has Varied and Changed : Findings and Summary of the U.s. Climate Change Science Program Synthesis and Assessment Product 1.3. *Climate Change Science Program.*

Allen, M. R. & Ingram, W. J. 2002 Constraints on future changes in climate and the hydrological cycle. *Nature,* **419** 224-232.

Benestad, R. E., Hanssen-Bauer, I. & Chen, D. 2008 Empirical-statistical downscaling. *World Scientific Publishing Company.*

Cai, S., William W., H. & Alex J., C. 2006 A comparison of bayesian and conditional density models in probabilistic ozone forecasting. *Hydrological Processes,* **16**, 1137-1150.

Barrow, E., Maxwell, B., Gachon, P. & Canada, C. E. 2004 Climate Variability and Change in Canada: Past, Present and Future. *Environment Canada.*

Beniston, M., Stephenson, D. B., Christensen, O. B., Ferro, C. A. T., Frei, C., Goyette, S., Halsnaes, K., Holt, T., Jylh, K. & Koffi, B.

2007 Future extreme events in european climate: an exploration of regional climate model projections. *Climatic Change,* **81 (S1)**, 71-95.

Bromwich, D. H. & Cullather, R. I. 1998 The atmospheric hydrologic cycle over the Arctic basin from ECMWF re-analyses. *Proc. of the WCRP First Int. Conf. on Reanalyses Silver Spring, MD, WCRP, in press.*

Cannon, A. J. & McKendry, I. 2002 A graphical sensitivity analysis for statistical climate models: Application to indian monsoon rainfall prediction by artificial neural networks and multiple linear regression models. *International Journal of Climatology,* **22**, 1687-1708.

Cannon, A. J. 2008 Probabilistic multisite precipitation downscaling by an expanded bernoulli-gamma density network. *Journal of Hydrometeorology,* **9**, 1284-1300.

Cannon, A. J. 2010 A flexible nonlinear modelling framework for non-stationary generalized extreme value analysis in hydro-climatology. *Hydrological Processes,* **24**, 673-685.

Cawley, G. C., Janacek, G. J., Haylock, M. R. & Dorling, S. R. 2007 Predictive uncertainty in environmental modelling. *Neural Networks,* **20 (4)**, 537–549.

CBCL Ltd. 2014 Rennies River Catchment Stormwater Management Plan. *CBCL Project No. 123097* .

Chen, D. & Hellström, C. 1999 The influence of the north atlantic oscillation on the regional temperature variability in sweden: spatial and temporal variations. *Tellus,* **51A**, 505-516.

Christopher, J. W., Sanabria, A, Corney, S, Grose, M, Holz, M, Bennett, J, Cechet, R & Bindoff, N.L. 2010 Modelling Extreme Events in a Changing Climate using Regional Dynamically- Downscaled Climate Projections. *IEMSs 2010 International Congress on Environmental Modelling and Software, Ottawa.*

Dawson, C. & Wilby, R. 2001 Hydrological modelling using artificial neural networks. *Progress in Physical Geography,* **25**, 80-108.

Christensen, J. H., Carter, T. R., Rummukainen, M. & Amanatidis, G. 2007 Evaluating the performance and utility of regional climate models: The PRUDENCE project. *Climate Change,* **81**, 1-6.

Dickinson, R.E., Errico, R.M., Giorgi, F.& Bates, G.T. 1989 A regional climate model for western United States. *Climatic Change,* **15**, 383-422.

Dorling, S., Foxall, R., Mandic, D. & Cawley, G. 2003 Maximum likelihood cost functions for neural network models of air quality data. *Atmospheric Environment,* **37(24)**, 3435-3443.

Finnis, J., Holland, M. M., Serreze, M. C. & Cassano, J. J. 2007 Response of Northern Hemisphere extratropical cyclone activity and associated precipitation to climate change, as represented by the Community Climate System Model. *Journal Geophysics Ressources,* **112** G04S42, doi:10.1029/2006JG000286.

Folland, C. & Karl, T. 2001 Observed climate variability and change. in: Houghton, j.t. et al., editors. climate change 2001: the scientific basis. *Cambridge University Pres,* , 99-181.

Forland, E.J., Engelen , A., Ashcroft, J., Dahlstrom, B., Demaree, G., Frich, P., Hanssen-Bauer, I., Heino, R., Jonsson, T., Mietus, M., Muller-Westermeier, G., Palsdottir, T., Tuomenvirta, H. & Vedin, H. 1996 Change in normal precipitation in the north atlantic region (2nd edn). *DNMI Report 7-96 Klima.*

Fowler, H. J., Blenkinsop, S.,& Tebaldi, C. 2007 Linking climate change modelling to impact studies: Recent advances in downscaling techniques for hydrological modelling. *International Journal Climatology,* **27**, 1547-1578.

Frei, C., Schar, C., Luthi, D. & Davies, H. C. 1998 Heavy precipitation processes in a warmer climate. *grl,* **25**, 1431-1434.

Frei, C., Schll, R., Fukutome, S., Schmidli, J. & Vidale, P. L. 2006 Future change of precipitation extremes in Europe: Inter-comparison of scenarios from regional climate models. *Journal of Geophysical Research,* 111.

Gardner, M. W. & Dorling, S. 1998 Artificial neural networks (the multilayer perceptron)a review of applications in the atmospheric sciences. *Atmospheric Environment,* **32**, 2627–2636.

Gautam, D. & Holz, K. 2000 Neural network based system identification approach for the modelling of water resources and environmental systems. *Artificial intelligence methods in civil engineering applications,* 87-100.

Giorgi, F. 1990 Simulation of regional climate using a limited area model nested in a general circulation model. *Journal of Climate,* **3**, 941-963.

Goodess, C. M. 2011 An inter-comparison of statistical downscaling methods for Europe and European regionsAssessing their performance with respect to extreme

weather events and the implications for climate change applications. *Technical report, Univ. of East Anglia, Norwich, U. K., in press.*

Groisman, P., Karl, T., Easterling, D., Knight, R. W., Jamason, P., Hennessy, R. S., C.M., P., Wibig, J., Fortuniak, K., Razuvaev, V., Forland, E. & Zhai, P. 1999 Changes in the probability of heavy precipitation: Important indicators of climatic change. *Climate Change,* **42**, 243-283.

Gutowski, W.J., Arritt, R.W., Kawazoe, S., Flory, D.M., Takle, E.S., Biner, S., Caya, D., Jones, R.G., Laprise, R., Leung, R.L., Mearns, L.O., Moufouma-Okia, W., Nunes, A.M.B.,Qian, Y , Roads, J.O., Sloan, L.C. & Snyder, M.A. 2010 Regional Extreme Monthly Precipitation Simulated by NARCCAP RCMs. *Journal of Hydrometeor,* **11**, 1373-1379. doi: http://dx.doi.org/10.1175/2010JHM1297.1

Haylock, M. R., Cawley, G. C., Harpham, C., Wilby, R. L. & Goodess, C. M. 2006 Downscaling heavy precipitation over the united kingdom: a comparison of dynamical and statistical methods and their future scenarios. *International Journal of Climatology,* **26**, 13971415.

Hellström, C., Chen, D., Achberger, C. & Risnen, J. 2001 Comparison of climate change scenarios for sweden based on statistical and dynamical downscaling of monthly precipitation. *Climate Research,* **19**, 45-55.

Hennessy, K. J. & Suppiah, R. 1999 Australian rainfall changes, 19101955. *Australian Meteorological Magazine,* **48**, 1-13.

Hostetler, S.W., Bartlein, P.J., Clark, P.U., Small, E.E. & Solomon, A.M. 2000 Simulated influence of Lake Agassiz on the climate of Central North America 11,000 years ago. *Nature,* **405(6784)**, 334–337.

Houghton, JT., Meira Filho, L.,Callander, B., Harris, N., Kat- tenberg, A. & Maskel, l. K. e. 1996 IPCC climate change. the IPCC second assessment report. *Cambridge University Press: New York .*

Hsieh, W. W. & Tang, B. 1998 Applying neural network models to prediction and data analysis in meteorology and oceanography. *Bulletin of the American Meteorological Society,* **79**, 1855-1870.

Hsieh, W. W. 2009 Machine Learning Methods in the Environmental Sciences. *Cambridge University Press,* **1st edition**.http://dx.doi.org/10.1017/CBO9780511627217.

Iwashima, T.& Yamamoto, R. 1993 A statistical analysis of the extreme events: long-term trend of heavy daily precipitation. *Journal of the Meteorological Society of Japan,* **71**, 637-640.

Kaas, E. & Frich, P. 1995 Diurnal temperature range and cloud cover in the nordic countries: observed trends and estimates for the future. *Atmospheric Research,* **37**, 211-228.

Kalnay, E., Kanamitsu, M., Kistler, R., Collins, W., Deaven, D., Gandin, L., & Joseph, D. 1996 The NCEP/NCAR 40-year reanalysis project. *Bulletin of the American meteorological Society,* **77(3)**, 437-471.

Kalnay, E 2003 Atmospheric Modeling, Data Assimilation and Predictability. *Cambridge university.*

Karl, T. R., Knight, R. W. & Plummer, N. 1995 Trends in high frequency climate variability in the twentieth century, 217-220.

Karl, T. R. & Knight, R. W. 1998 Secular trends of precipitation amount frequency and intensity in the United States. *Bulletin of the American Meteorological Society,* **79**, 231-241.

Kaas, E. & Frich, P. 1995 Diurnal temperature range and cloud cover in the nordic countries: observed trends and estimates for the future. *Atmospheric Research,* **37**, 211-228.

Lenderink, G., Buishand, A. ,& van Deursen, W. 2007 Estimates of future discharges of the river Rhine using two scenario methodologies: Direct versus delta approach. *Hydrology and Earth System Sciences,* **11(3)**, 1145-1159.

Linderson, M., Achberger, J. & Chen, D. L. 2004 Statistical downscaling and scenario construction of precipitation in scania, southern sweden. *Nordic Hydrology,* **35(3)**, 261-278.

Mekis, & Vincent, L.A. 2011 An overview of the second generation adjusted daily precipitation dataset for trend analysis in Canada. *Atmosphere-Ocean,* **49(2)**, 163-177.

Plummer, N., Salinger, M. J., Nicholls, N., Suppiah, R., Hennessy, K. J., Leighton, R. M., Trewin, B., Page, C. M. & Lough, J. M. 1999 Changes in climate extremes over the australian region and new zealand during the twentieth century. *In Weather and Climate Extremes,* 183-202. Springer Netherlands.

Rummukainen, M. 1997 Methods of statistical downscaling of GCM simulations. *SMHI Rapporter. Meteorologi och Klimatologi (Sweden). no.* **80**.

SAS Institute Inc. 2011 SAS(R) Enterprise Miner 7.1 Extension Nodes: Developers Guide. *SAS Cary, NC: SAS Institute Inc.*

Sc̈honwiese, C. & Rapp, J 1996 Climate trend atlas of Europe based on observations 1891- 1990. *Kluwer Academic Publishers: Dordrecht.*

Schoof, J. & Pryor, S. 2001 Downscaling temperature and precipitation: a comparison of regression-based methods and artificial neural networks. *International Journal Climatology,* **21**, 773–790.

Suppiah, R. & Hennessy, K. J. 1995 Trends in the intensity and frequency of heavy rainfall in tropical Australia and links with the southern oscillation. *World Meteorological Organization-Publications-WMO TD,* 897-901.

Suppiah, R. & Hennessy, K. J. 1998 Trends in total rainfall, heavy rainfall events and number of dry events in Australia, 1910-1990. *International Journal of Climatology,* **18**, 1141-1164.

Trenberth, K.E., Karl, T. R. & Knight, R. W. 2003 Modern global climate change. *Science,* **302**, 1719-1723

Vincent, L. A. 1998 A technique for the identification of inhomogeneities in Canadian temperature series. *Journal of Climate,* **11**, 1094-1104.

Vincent, L. A. & Gullett, D. W. 1999 Canadian historical and homogeneous temperature datasets for climate change analyses. *International Journal of Climatology,* **19**, 1375-1388.

Vincent, L. A., Zhang, X., Bonsal, B.R. & Hogg, W. D. 2002 Homogenization of daily temperatures over Canada. *Journal of Climate,* **15**, 1322-1334.

Vincent Lucie, A. & Mekis, V.A. 2006 Changes in daily and extreme temperature and precipitation indices for canada over the twentieth century. *Atmosphere-Ocean,* **44 (2)**, 177-193.

Vrac, M., & Naveau, P. 2007 Stochastic downscaling of precipitation: From dry events to heavy rainfalls. *Water resources research,* **43(7)**.

Weichert, A.& Bu̎rger, G. 1998 Linear versus nonlinear techniques in downscaling. *Climate Research,* **8**, 83-93.

Wigley, T. M. L., Jones, P. D., Briffa, K. R. & Smith, G. 1990 Obtaining subgrid scale information from coarse resolution general circulation model output. *Journal of Geophysical Research: Atmospheres (1984-2012),* **95(D2)**, 1943-1953.

Wilby, R. L., Wigley, T. M. L., Conway, D., Jones, P. D., Hewitson, B. C., Main, J.& Wilks,D. S. 1998 Statistical downscaling of general circulation model output: A comparison of methods. *Water resources research,* **34(11)**, 2995-3008.

Wilks, D. S. 1998 Multisite generalization of a daily stochastic precipitation generation model. *Journal of Hydrology,* **210**, 178–191.

Wilks, D. S. 2006 Statistical Methods in the Atmospheric Sciences. *Academic Press,* **627**.

Williams, P. M. 1998 Modelling seasonality and trends in daily rainfall data. *Prameters,* **16(12)**, 15.